21st Australasian Fluid Mechanics Conference
Adelaide, Australia
10-13 December 2018

Investigating the Flow Effects of Slots and Perforations on a Flat Blade

M. L. Toole, R. M. Kelso, and C. Birzer

School of Mechanical Engineering
Unversity of Adelaide, South Australia 5005, Australia

Abstract

The following study investigates the flow effects caused by slots and perforations on a flat blade for use in a simple, undershot, water-wheel to better understand the flow mechanics of these turbines. This study has a primary aim of increasing the power generated by these blades without significantly increasing manufacturing costs. Experimental tests were conducted in a wind tunnel with 2.4% blockage ratio. These tests aimed to measure the power coefficient of the blade over a range of flow velocities and angles of attack. Reynolds Number matching was used to ensure that the use of a wind tunnel for a water-based design was adequate. Initial tests were undertaken on four designs with similar porosity ratios. After the initial results were found, these designs evolved to find an optimal solution. The results show that, under the test conditions, the square slotted design with porosity, ϕ, of 0.1 was optimal. It provided a slight increase in overall power coefficient at high angle of attack while using 10% less manufacturing material. The final design also improved downstream flow effects, causing a more rapid decay in the wake velocity. This increases the power generation of blades further downstream when used in a turbine configuration. Collectively, these results provide an insight into the flow effects of perforated and slotted flat blades in a controlled experimental environment, which will be used in the future to improve the design of the simple water-wheel.

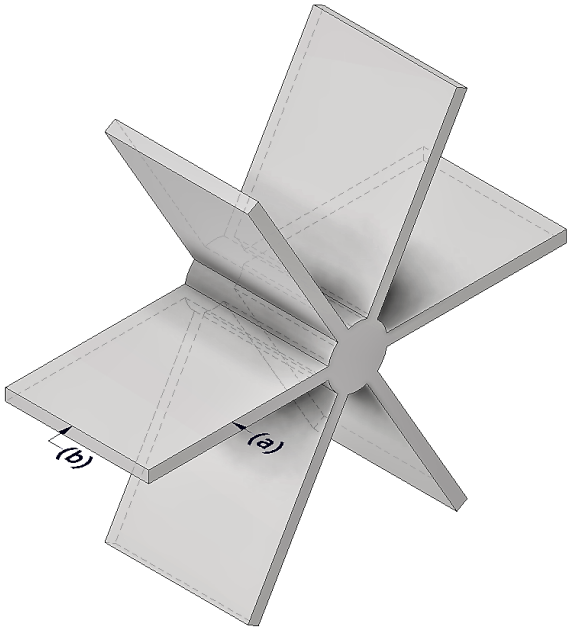

Figure 1: Full assembly of simple undershot water-wheel with blade length (a) and width (b)

Introduction

Interest in the development and improvement of the simple water-wheel has grown in the last few years, with studies like Batten et al. (2011) [1], Castro-Garcia et al. (2015) [2] and Nguyen et al. (2018) [5], providing valuable technical analysis of the structure or discussing the improvement of several components — such as the flotation device, the number of blades and the shape of the blades. The aim of the study is to add to this body of work by investigating slots and perforations. The results found in these recent studies, as well as the results of this study, will be used to begin to determine an optimal design (or design method) for undershot water-wheels. Batten et al. (2011) [1] discussed the design and stability of a free stream energy converter with a design similar to the turbine seen in figure 1. This paper discussed implementing more effective flotation devices to better control the depth ratio of the system. Castro-Garcia et al. (2015) [2] performed an analysis of the Albolafia water-wheel in Spain, a water-mill from the middle ages. This paper offered an insight into the modelling and functional analysis of a water-wheel. While this paper focussed on a historical model of the water-wheel, many of the characteristics investigated remain relevant in more modern systems. Nguyen et al. (2018) [5] provided an in-depth analysis on the flow fields generated by a water-wheel using experimental and numerical tests. This study indicates that the development of water-wheels is ongoing and that with optimization can be used as a viable power generation method. Most experimental studies on the effects of perforations and slots on flat blades (or plates) have been conducted under a different setting with largely different design parameters and goals. Analysis in Dong, et al (2008) [3], investigated the drag force and moments of upright fences under several different wind velocities and fence porosities. While the application is drastically different, some of the underlying fluid mechanics are similar. The tests by Dong et al. were aiming to reduce the velocity of the wind downstream, since that is the purpose of a wind fence. In the current study, the aim is to maximise the drag force and therefore the force generation. Interestingly, the study by Dong et al. found that the drag and moment coefficients of the fence were almost independent of the Reynolds Number over the tested range from 10,000 to 18,000. They found that the largest changes in the drag and moment coefficients were most likely caused by vertical wind speed variations near the fence. The study concluded with the finding that a fence with porosity between 0.3 and 0.4 had the largest drag coefficient and moment, which corresponds to the greatest reduction in downstream wind speeds due to energy dissipation caused by the turbulence in the wake. However, these fence systems are significantly different to the blades presented in the current study. The fences were made with vertical steel wires, placed at different spacings to adjust the porosity easily.

Experimental Method

The experimental testing was undertaken in an open-jet wind tunnel with nominal nozzle dimension of 0.5m by 0.5m. To simulate a partially submerged blade in water, the blade was positioned with a floor boundary to simulate the free surface that would occur between water and air. Corrections derived from an earlier body of work (Hansen, 2012 [4]) using this wind tunnel were used to ensure that this experimental method

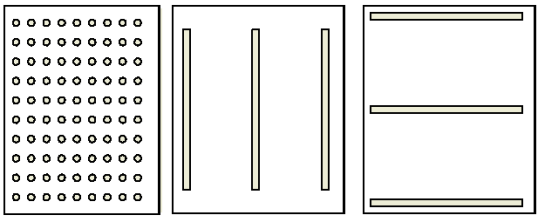

Figure 2: First Iteration Designs

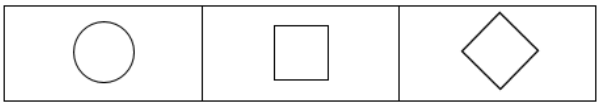

Figure 3: Perforation Shapes used in testing

simulated the real case effectively; the boundary layer and momentum thickness of the system are both under 10mm at the blade position. Four initial designs were tested over a range of velocities, from 0-20m/s. Using Reynolds number matching, these wind velocities correlate with a water velocity range of 0-1.4m/s. The Reynolds number in these experiments range from 0 to $1.6 * 10^5$. These four initial designs were: the base case, 5mm diameter holes, horizontal slots and vertical slots. The base case refers to the design with no perforations or slots. These designs can be seen in figure 2. Each of these designs had nominal dimensions 120mm x 150mm, and were tested at a porosity ratio (ϕ) of 0.1. The blade designs had a thickness of 5mm, which was required for stability during the tests but may affect drag force produced at low angles of attack. The drag force on the blade was measured using a single axis load cell of tolerance class 0.02%, and the data was analysed using LoadVUE software. This data was gathered at a sampling frequency of 500 Hz over a 20 second sampling time. Once data was gathered for these original designs over a range of wind velocities, the most appropriate slot and perforation configuration was further iterated to attempt to find the optimal porosity ratio. These iterated designs were tested in a similar way over a range of velocities and angles of attack as defined in figure 4. The remainder of the tests were undertaken using slotted designs at various porosity values and shapes, namely: ϕ = 0.05, 0.1 and 0.15 with circular, square and diamond shaped perforations (see figure 3). Each shape had an equal area to maintain the porosity ratios across tests. The square and diamond had equal aspect ratios. The perforations were all distributed across the blades evenly.

To determine the coefficient of power (C_P) for a given system layout, the power potential in the wind has to be defined. The coefficient of power is generally defined by the following equation:

$$C_P = \frac{P_{OUT}}{P_{IN}} \tag{1}$$

where P_{OUT} is derived from the value, F, from the load cell:

$$P_{OUT} = FV \tag{2}$$

where V is the free-stream jet velocity of the wind generated by the wind tunnel. P_{IN} is defined as

$$P_{IN} = \frac{1}{2}\rho(1-\phi)abV^3. \tag{3}$$

Here, ρ is defined as the density of air, ϕ is the porosity, a is the length of the blade, and b is the width of the blade.

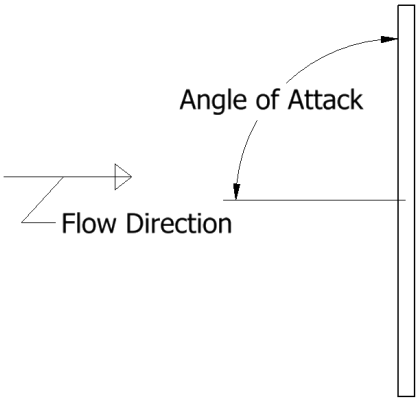

Figure 4: Definition of angle of attack for experimental set-up

Results

The initial test results can be seen in figure 5, which compares the power coefficient results over a range of velocities at $\alpha = 90°$. These results indicate that the slotted blades performed worse than the perforated blade and the base case. The lower power coefficient may be attributed to a less effective distribution of fluid flow over the face of the blade.

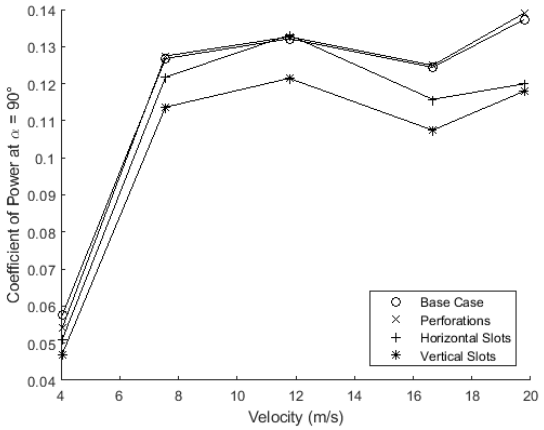

Figure 5: Summary of Initial Tests comparing Slots and Perforations at ϕ = 0.1 and $\alpha = 90°$

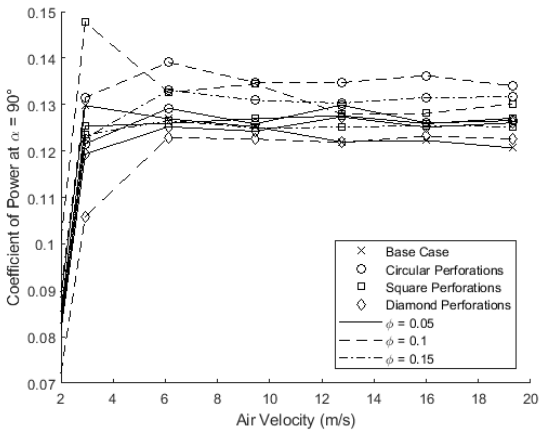

Figure 6: Comparison of Slot sizes and shapes at $\alpha = 90°$

Figure 6 shows the results of the perforation tests at $\alpha = 90^\circ$. While most designs operated similarly at higher velocities (from 8m/s) some designs had noticeably better or worse results at low wind speeds. The design with the best performance at low wind speeds had square perforations at $\phi = 0.1$. Most others performed at a similar level, but the worst performing was the diamond shaped perforation design at $\phi = 0.1$. It is likely that different shapes have different Reynolds number dependency and flow characteristics through the perforations.

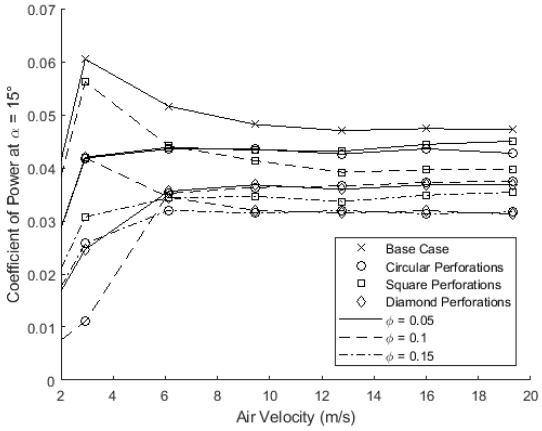

Figure 7: Comparison of Slot sizes and shapes at $\alpha = 15^\circ$

Figure 7 shows similar results to figure 6 but at the lowest angle of attack tested, $\alpha = 15^o$. As expected, the coefficient of power decreases as the angle of attack decreases due to a lower frontal area for the blade. Figure 7 indicates all designs still operated similarly at higher velocities, as per figure 6. However, figure 7 has a significantly higher variance at all velocities when compared to figure 6. Under these test parameters, the base case performed best, followed by the square perforation design with $\phi = 0.1$. The worst performing designs were the circle and diamond design at $\phi = 0.1$ and the circle design at $\phi = 0.1$. These two figures would indicate that the square perforated design at $\phi = 0.1$ performs best, while most designs fall in a similar range below the base case. Figure 8 is a similar graph at $\alpha = 45^\circ$. This graph has a similar shape to figure 6 with similar results; in this case, however, the base case performs better than any other designs.

The results shown in figures 6, 7 and 8 allow some analysis to

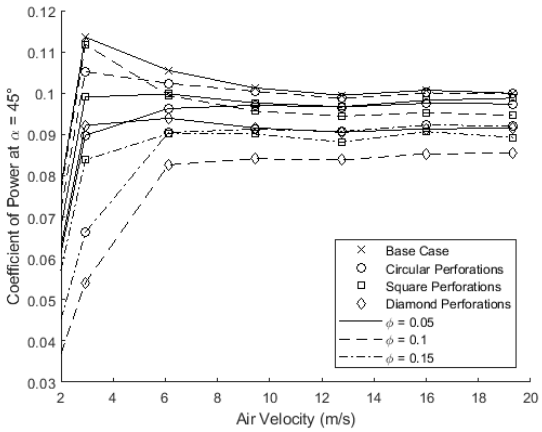

Figure 8: Comparison of Slot sizes and shapes at $\alpha = 45^\circ$

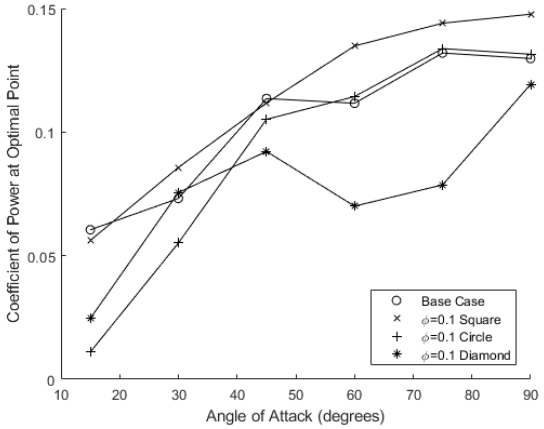

Figure 9: Comparison of Coefficients of Power at varying α for $\phi = 0.1$

be made regarding which designs operate best and which operate poorly. The best performing non-base case design is the square perforated design at $\phi = 0.1$. The results indicate that at the lowest porosity ratio tested, 0.05 has a minimal impact on the coefficient of power of the blade at any angle of attack or velocity, with most results performing similarly to the base case or marginally worse. Since the porosity ratio of 0.05 is so low, the blade simply performs as if it had 0 porosity in many cases. This is also partially attributed to the thickness of the blade being 5mm, which was necessary to test at higher wind speeds. Since in some cases, the thickness of the plate is approximately equal to the hole diameter, the flow most likely separates as it enters the holes before reattaching. This leads to some Reynolds number dependence. A porosity ratio of 0.15 generally causes the blade to perform worse at low fluid velocities while offering a slight improvement at higher velocities when compared to the base case. This may be attributed to the larger perforations allowing a significant amount of fluid through the blade, and thus, not contributing to the overall power generated by the blade. This effect is more noticeable (and detrimental) at lower velocities while at higher velocities the effect is minimised.

In terms of the different shapes used as perforations, the results indicate that the square performed best. The circle perforations performed similarly to the base case, generally, while the diamond perforations performed the worst. Since, in all cases, the perforation shapes were distributed across the blade evenly (i.e. each design had their perforation shapes centred around the same points), the change in the power coefficient caused by each shape is attributed to the edge distance between each perforation. The square designs had the most consistent edge distance between perforations while the circle and diamond perforations had larger distances, causing the fluid to be distributed inefficiently.

Figure 9 shows the change in the coefficient of power while varying the angle of attack and maintaining a porosity ratio of 0.1. This graph illustrates how the blade perforation shape influences the power generated over a range of angles. While the blades performed similarly at low angles of attack, this graph demonstrates that at higher angles of attack (and higher coefficients of power) the diamond blade performed poorly.

Conclusions

The primary aim of this investigation was to determine whether the use of slots and perforations improved the performance of an undershot water-wheel. The use of slots and perforation were

also theorised to reduce the turbulence as water flows past the wheel, thus increasing the generating efficiency of the downstream blades. Test were undertaken in a small-scale wind tunnel to ease the testing method when compared to full-scale water testing. A broad range of configurations were tested, with variations made to the: blade perforation shape, wind velocity and angle of attack. The results of the testing indicated that the use of slots and perforations, in most cases, reduce the power generated by an amount proportional to the amount of material removed by the slots or perforations (e.g. a 5% porosity ratio correlates to a 5% decrease in power output). However, some designs performed better than the base case at certain angles of attack and velocities. For example, the square perforated design at $\phi = 0.1$ generated a higher coefficient of power than the base case at all angles of attack greater than 45°. These results will be used to influence a future body of work that focuses on the overall improvement and modernisation of undershot waterwheels.

Acknowledgements

The first author gratefully acknowledges the funding received from the federal government under the Research Training Program. The authors also thanks the University of Adelaide for providing facilities throughout the study.

References

[1] Batten, W.M.J., Weichbrodt, F., Muller, G.U., Hadler, and others, Design and stability of a floating free stream energy converter, *Proceedings of the 34th World Congress of the International Association for Hydro-Environment Research and Engineering: 33rd Hydrology and Water Resources Symposium and 10th Conference on Hydraulics in Water Engineering*, 2011.

[2] Castro-Garcia, M. Rojas-Sola, J.I., and others, Technical and functional analysis of Albolafia waterwheel (Cordoba, Spain): 3D modeling, computational-fluid dynamics simulation and finite-element analysis, *Energy Conversion and Management*, 2015.

[3] Dong, Z., Mu, Q., Luo, W., Qinan, G., and Lu, P., and Wang, H., An analysis of drag force and moment for upright porous wind fences, *Journal of Geophysical Research: Atmospheres*, 2008.

[4] Hansen, K.L., Effect of leading edge tubercles on airfoil performance, PhD Thesis, *University of Adelaide*, 2012.

[5] Nguyen, M.H., Jeong, H. and Yang, C., A study on flow fields and performance of water wheel turbine using experimental and numerical analyses, *Science China Technological Sciences*, 2018.